Selective Deposition of Metal Nanoparticles Inside or Outside Multiwalled Carbon Nanotubes

Jean-Philippe Tessonnier,[†] Ovidiu Ersen,[‡] Gisela Weinberg,[†] Cuong Pham-Huu,[§] Dang Sheng Su,[†,*] and Robert Schlögl[†]

[†]Fritz-Haber-Institut der Max-Planck-Gesellschaft, Faradayweg 4-6, 14195 Berlin, Germany, [‡]Institut de Physique et Chimie des Matériaux de Strasbourg, UMR 7504 du CNRS, 23, rue du Loess, 67087 Strasbourg, France, and [§]Laboratoire des Matériaux, Surfaces et Procédés pour la Catalyse, UMR 7515 du CNRS, 25, rue Becquerel, 67087 Strasbourg, France

ABSTRACT A general method is described for the deposition of metal nanoparticles selectively either inside or outside of carbon nanotubes (CNTs). The method is based on the difference in the interface energies of organic and aqueous solutions with the CNT surface. Because of their lipophilic character, the organic solvent better wets the surface of the nanotubes compared to water and penetrates into the inner volume. The precise control of the volume of each phase allows filling the CNT with the organic phase and covering its outer surface with the aqueous one. Hence, metal nanoparticles can be put with high selectivity either inside or outside the CNT, just by choosing in which solvent the metal precursor is dissolved. SEM, TEM, and 3D-TEM investigations show that a selectivity in localization close to 75% can be reached by this technique. The nanoparticles are homogeneously dispersed and present a narrow size distribution, centered on 5 nm. In this way, one can decorate either the inner or the outer surface of open CNTs, without the need of discriminating the diameter of the opening and without any further step of functionalization than a treatment with nitric acid.

KEYWORDS: carbon nanotube · nanoparticles · deposition · confinement · electron tomography

Carbon nanotubes (CNTs) present exceptional physical properties that make them suitable for applications in very different fields like medicine, electronics, polymers, or catalysis.[1−3] Their exceptional mechanical, thermal, and electronic properties, along with the possibility to chemically modify their surface by doping or grafting,[4,5] make them a platform for various applications. In the early days of their discovery, several groups studied the filling of multiwalled carbon nanotubes (MWCNTs) with metals, metal alloys, and even metal oxides.[6,7] The filling was performed on the basis of the capillary forces that suck a molten salt or a solution containing a metal precursor inside the tubule.[8] This technique was further developed and used to investigate the properties of a large range of confined materials, including metal oxide nanoparticles,[9] magnetic nanoparticles,[10] fluorescent nanoparticles,[11] ionic liquids,[12] organometallic molecules,[13] polymers,[14] C_{60},[15] and even carbon nanofibers.[16] It allowed the investigation of properties of materials when nanosized.[17]

Catalysis witnessed a real explosion in investigations using carbon nanotubes as catalyst support. The early synthesis methods invented to prepare metal/metal oxide nanowires were successfully used to decorate the CNTs with nanoparticles, thus using CNTs as catalyst support.[2] It is worth noting that CNT-based catalysts often show higher activity and/or selectivity than catalysts made of the same active phase but deposited on other supports, like alumina, silica, or even activated carbon.[2,18] The reasons for this particular behavior are their particular electronic properties, their high thermal conductivity, the high accessibility of the active phase, and the absence of any microporosity, thus eliminating diffusion and intraparticle mass transfer limitations. Much work has been done since then to optimize the decoration of the CNTs in terms of dispersion and control of the particle size distribution. The techniques developed allow the attachment of nanoparticles to the CNT surface without distinction between inner and outer surface, that is, inside or outside the tubular structure. Several groups however suggested that the curvature and the aspect ratio of the tubes might play some role on the catalytic properties of the metal nanoparticles.[2,19−21]

The curvature affects the metal−support interaction and the electronic structure of the metal and hence its catalytic activity. The resulting double-bond localization of π electron density as compared to graphite enhances the s-character of the carbon−carbon bond compared to a planar sp^2 interaction.[22] On the other hand,

*Address correspondence to dangsheng@fhi-berlin.mpg.de.

Received for review June 19, 2009 and accepted July 20, 2009.

Published online July 27, 2009.
10.1021/nn900647q CCC: $40.75

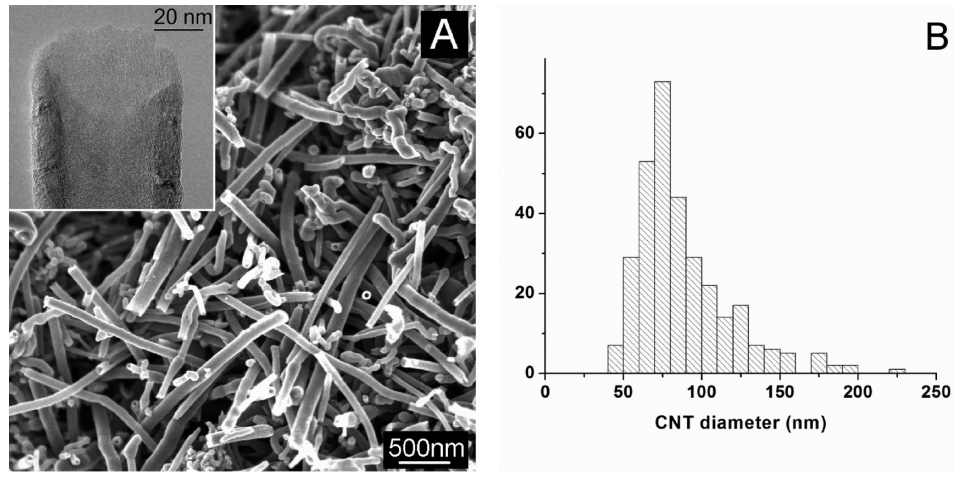

Figure 1. (A) SEM image of the pristine CNTs. Inset: HRTEM image of a CNT tip. (B) Statistical distribution of their outer diameter.

the tubular inner core is expected to yield to confinement effects similar to those existing inside the pores of zeolites.[23] Diffusion of molecules inside wide pores happens similarly to water flowing through a pipe. It conventionally takes place following the Poiseuille mode of diffusion, where molecule−molecule collisions are much higher than molecule−wall collisions. When the size of the pore or of the pipe decreases, the interaction of the molecules with the walls cannot be neglected anymore.[24] The flow then follows the Knudsen model. If the size of the pore is further decreased to reach the dynamic diameter of molecules in the gas phase, particular effects due to confinement of the molecule in the pore appear.[25] These effects are well-known in the case of zeolites which present cavities in the range of 1−10 Å. They are extensively described in the review of Derouane.[23] The existence of similar effects in larger pores, that is, in the nanometer range, was a matter of debate during several years. Recently, it was however demonstrated that they also exist in organized mesoporous silicates like MCM-41 and SBA-15 that present pores of few nanometers.[26] Similar effects are thus suspected to also exist inside CNTs.

To access this information and to be able to perform an investigation of the catalytic properties of metals inside or outside CNTs, one has to first master the synthesis of metal nanoparticles selectively localized inside or outside of carbon nanotubes. Several groups already attempted such localized selective deposition. Two main synthesis routes were suggested: (1) *Deposition on CNTs of various diameters.* It has been observed that wetting and filling of the inner tubule becomes difficult if not impossible for CNTs with diameters below 30 nm. On the basis of this observation, Ma *et al*. decorated CNTs of different diameters with Pt, inside for large CNTs, outside for smaller ones, and tested the catalytic activity for cinnamaldehyde hydrogenation.[27] A variation of the catalytic behavior was reported. Unfortunately, by varying the tube diameter, both the curvature and the size of the inner cavity are changed, and hence no curvature/confinement effects can be deduced from the catalytic behavior. (2) *Asymmetric functionalization*. The first asymmetric functionalization was reported by Lee *et al*. who managed to graft different functional groups on each tip of the same CNT.[28] A similar concept was used by Jiang *et al*. to perform the asymmetric functionalization of the inner and outer surface of opened CNTs.[29] Chen *et al*. used oxidation with nitric acid to functionalize caped CNTs and, depending on the reaction conditions, to selectively open their ends.[30] Functionalization deeply modifies the surface properties of the CNTs. However, none of these reports mentions effects on supported metal nanoparticles.

The characterization of the sample is not straightforward with respect to the localization of the supported metal nanoparticles. Winter *et al*., as well as Ersen *et al*., demonstrated that metal nanoparticles supported on CNTs are difficult to localize from conventional single view TEM images because of ambiguous estimates of projection effects.[31,32] It is nearly impossible to determine the 3D location in a 2D image for particles that appear to be in the center of the tube or next to the inner wall of the tube without tilting the specimen in the TEM. Electron tomography (3D TEM) appears to be a suitable technique that can clearly evidence the exact location of the particle with respect to the nanotube and further yields some statistics about the ratio of particles inside and outside the CNTs.

We present a novel and efficient method for decorating carbon nanotubes with metal nanoparticles. This method is based on the difference in the liquid/solid interface energies of an aqueous and an organic solution with the CNT surface. The efficiency of this method to localize nanoparticles has been checked by SEM, TEM, and 3D-TEM. This novel synthesis method allows a selective localization of nanoparticles inside or outside CNTs and thus the investigation of possible cur-

vature or confinement effects on the catalytic activity of transition metal nanoparticles.

RESULTS AND DISCUSSION

Structure and Chemistry of the CNT Support. The morphology of the starting CNTs was first checked by SEM and TEM. The images show that the pristine MWCNTs have both ends opened and present lengths up to several micrometers (Figure 1). Statistical analysis, performed by measuring more than 300 tubes on calibrated SEM images, reveals that they exhibit an outer diameter of 90 ± 30 nm. TEM images (inset of Figure 1A) show that their wall thickness ranges between 5 and 20 nm, thus leaving an empty channel of 20 to 50 nm. Their large inner diameter facilitates the filling of the CNTs with either organic or aqueous solutions. It is reported that metal nanoparticles are mainly deposited outside CNTs when their inner diameter is below 20−30 nm.[27,32] Thus, we use CNTs with large diameters to demonstrate the choice of localization of metal particles inside or outside by selecting the appropriate conditions of solvents. This allows us to rule out exclusion effects of the CNT diameter on the localization of the deposits. Hence, we make sure that the localization is only controlled by the synthesis conditions.

Although the starting commercial CNTs were already purified and opened, HNO_3 treatments were used to create a variety of oxygen containing functional groups on the sidewalls of the CNTs (Supporting Information). As the starting nanotubes are already opened, the nitric acid can wet and funtionalize the inner wall and the outer wall of the CNTs simultaneously. In addition, functionalization was done at 373 K with an excess of nitric acid (500 mL for 10 g CNTs) over 16 h to rule out any differences between functionalization of the inner and the outer surfaces due to diffusion limitations. In these mild conditions, we did not observe any weight loss which would be an indication for burnoff.

The functional groups were characterized by XPS and TG/TDS (Supporting Information). The surface composition calculated from XP spectra was found to contain 80 atom % C and 20 atom % O, thus confirming that the surface has been extensively functionalized. CO and CO_2 profiles obtained during TDS exhibit several peaks, representative of the variety of functional groups. CO_2 desorption was reported to arise from the loss of carboxylic acid, carboxyl anhydride, and lactone groups, whereas CO desorption originates from carboxyl anhydride, phenol, carbonyl, and ether groups.[33,34] The general shape of the TDS curves between 500 and 850 K indicate the presence of many acidic groups, in agreement with previous work.[33] Zeta potential measurement (Supporting Information) confirms the preeminence of strong acidic groups, as the zeta potential remains negative over the whole pH scale from pH 1.5 to 9.5. Deprotonation of the functional groups occurs whenever the HNO_3-treated CNTs are in contact with water, thus leaving a negatively charged carbon surface. This surface charge improves significantly the interaction between the CNT and metal cations of the precursors used during the subsequent impregnation. The functional groups attract the M^{x+} ions and help their dispersion, thus leading to metal nanoparticles evenly decorating the CNTs after calcination and reduction.

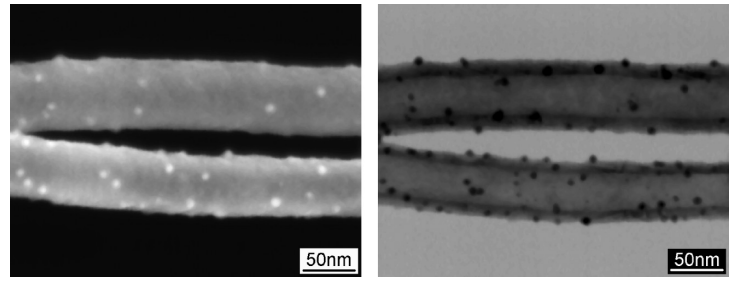

Figure 2. SEM images of the 1 wt % Ni/CNT sample prepared by incipient wetness impregnation. The same area was acquired in SE (left) and TE (right) mode.

Selective Deposition of Metal Nanoparticles Inside CNTs. Incipient wetness impregnation is a well-known technique used for catalyst preparation.[35] A solid catalyst support is brought in contact with a solution containing the metal precursor. The volume of this solution is adjusted to the porous volume of the solid so that it totally fills the pores, leaving the external surface almost dry. This technique usually leads to a homogeneous metal deposition, with a good dispersion and a narrow particle size distribution.[2] As most of the solution is located in the pores during the impregnation process, it is expected that most of the formed metal nanoparticles will be inside the nanotube. Recently, Ersen *et al.* investigated samples prepared by incipient wetness impregnation using tomography, that is, 3D-TEM.[32] A 2D-TEM image that shows particles only in the middle of the tube could be interpreted as all the particles being inside the CNT. However, 3D-TEM investigation of the same areas shows that these particles are actually above and below the central channel. For example, a 3D-TEM investigation of a Pd/CNT sample prepared by impregnation, using the same commercial CNTs as in the present study, presented almost 50% of the particles on the outer surface. We prepared a 1 wt % Ni on CNT sample by incipient wetness impregnation as reference. After impregnation, the sample was dried at 323 K for 10 h, then calcined in air at 623 K for 2 h, and finally, it was reduced in pure hydrogen at 673 K for 2 h. Figure 2 shows the SEM images obtained in SE and in TE mode. The TE detector of the SEM provides similar images as a TEM but with lower resolution. The main advantage compared to the TEM is that the same area can be easily imaged in SE and TE mode at the same time. This technique is particularly useful for CNTs decorated with metal nanoparticles as it provides simultaneously

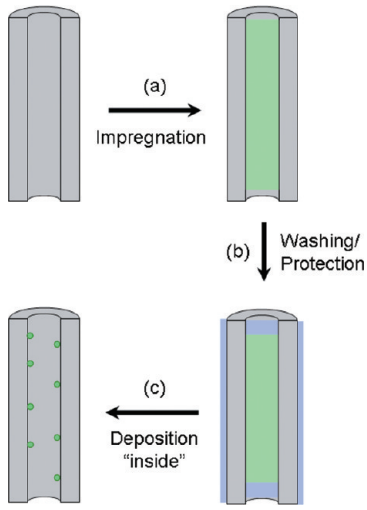

Scheme 1. Schematic view of a longitudinal cross section of a carbon nanotube during the different steps for the selective deposition of nanoparticles *inside* CNTs: (a) impregnation with the ethanolic solution containing the metal precursor; (b) impregnation with distilled water to wash and protect the outer surface from metal deposition; c) after drying, calcination, and reduction, metal particles are decorating the inner surface of the CNT with a high selectivity.

an image of the external surface and an image of the inner tubule. Figure 2 shows that many particles are located outside the CNT, in agreement with Ersen *et al.* We believe that during the incipient wetness impregnation process, the aqueous solution containing the Ni precursor mainly fills the inner channel. However, as the surface tension of water (72 $mN \cdot m^{-1}$) is lower than the critical surface tension of the CNTs (180 $mN \cdot m^{-1}$),[36] wetting of the CNT surface with the Ni precursor solution cannot be avoided. The external surface of the CNTs is also covered with solution, which leads after drying to the calcination and reduction of Ni nanoparticles on the outer surface.

We based our new synthesis procedure on the ideas that (i) the CNT has a better affinity for organic solvents, (ii) a solvent with a low surface tension (defined as the surface energy of the liquid per unit area when in contact with air) will easily wet and penetrate inside the CNT, and (iii) a second, metal-free, solvent will remain outside of the nanotube and protect its outer surface from metal deposition if the liquid/solid interface energy is higher than the first solvent. Thus, we performed a two-step synthesis (Scheme 1): 1 g CNTs are first impregnated with an ethanol solution containing the nickel nitrate precursor. The volume of the solution was set to be lower than the porous volume of the CNT (4 mL/g_{CNT} instead of 6 mL/g_{CNT}). Indeed, the porous volume of the CNTs originates from their inner channel but also from the entanglement of the nanotubes, which creates aggregated pores. These pores also contribute to the total pore volume of the CNTs. Using a volume of solution lower than the total pore volume was expected to favor the filling of the CNTs over the filling of the aggregates pores, which correspond to the external surface of the CNTs. Hence, a higher selectivity was expected. Because of its low surface tension (22 $mN \cdot m^{-1}$), the ethanolic solution wets the nanotube surface and fills the inner channel, as described by the Young−Laplace equation.[36] In a second step, 3 mL of pure distilled water are then added. The functionalization step with nitric acid created many oxygen-containing groups which decrease the hydrophobic character of the CNT surface and allow its wetting with both organic and aqueous solvents (contact angle $\theta < 90°$). However, the intrinsic lipophilicity of the nanotubes leads to lower liquid/solid interface energies for organic solvents than for aqueous ones. Therefore the aqueous phase is expected to remain outside of the nanotube and to displace the thin film of ethanolic solution located on the outer surface to the inner channel. The sample is dried at room temperature overnight and then at 323 K for 10 h to remove any remaining ethanol. The sample is finally calcined in air at 623 K for 2 h and reduced in pure hydrogen at 673 K for 2 h, as for the reference sample prepared by the incipient wetness method. TEM investigation (Figure 3) indicates that almost all the Ni nanoparticles are located inside the CNTs. SEM performed at low accelerating voltage (surface sensitive) shows however that some particles can still be found on the outer surface, hence proving that conclusions established from TEM about the location of metal nanoparticles on CNTs should always be supported by another technique like SEM or 3D-TEM.

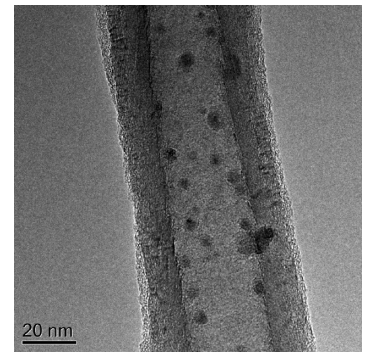

Figure 3. Representative TEM image of the sample "metal inside" prepared by 2-step impregnation. Most of the Ni nanoparticles seem to be inside the tubule.

Selective Deposition of Metal Nanoparticles outside CNTs. Decoration of the outer surface of closed CNTs is an easy task. However, decorating selectively only the outer surface of opened CNTs is far more challenging. It is reported that filling nanotubes with a solution becomes more difficult when the diameter of the CNT decreases.[27] For instance, small CNTs with diameters below 30 nm could not be filled with a solution; consequently decoration occurred only on the outer surface.[27] However, in our present work we used large CNTs for which we already demonstrated that they can be totally filled with any solution. The strategy in the present work is slightly different: the inner channel

needs to be protected during the impregnation with the solution containing the metal precursor. Consequently, the two-step impregnation is as follows (Scheme 2): we first perform an incipient wetness impregnation with an organic solvent A. This solvent has a low surface tension and consequently wets and fills the tubes easily. An aqueous solution B which contains the metal precursor is then added. Because of its higher liquid/solid interface energy, this solution cannot penetrate the CNTs. Thus, the channel remains protected and decoration only happens on the outer surface. This procedure might however not be obvious as its efficiency depends on the balance of all the interface energies, that is, liquid/solid for each of the solvents but also liquid/liquid. Several parameters might influence the choice of the solvent A. In particular, its miscibility with water and its boiling point might be two critical factors. In the first case, the aqueous solution might penetrate into the tubes by diffusing into the organic solvent. In the second case, if the organic solvent evaporates faster than the aqueous solution, the later might be able to enter the tubes. In both cases, it would result in an unselective decoration. In the present work, we tested solvents with different boiling points and miscibility with water (Table 1). At least two different solvents were tested for each couple of parameters, that is, octane and ethylbenzene for high boiling point/low solubility, benzene and trichloromethane for low boiling point/low solubility, *etc*. For each organic solvent listed in Table 1, we first impregnated 1 g of CNTs with a volume of this solvent (solvent A) corresponding exactly to the total pore volume of the nanotubes (6 mL/g_{CNT} in the present case). Organic solvents often have a high vapor pressure; their evaporation is fast. Therefore, the solvent A is put in excess in order to guarantee the complete filling of the CNTs and the protection of the inner tubule from metal deposition. In a second step, each sample was impregnated with the aqueous solution containing the Ni precursor. Finally, all samples were dried, calcined, and reduced in the same conditions as previously. The SEM investigation at low accelerating voltage shows that small nanoparticles are homogeneously decorating the outer surface of the CNTs (Figure 4). The choice of the solvent A affected neither the Ni particle dispersion on the CNT support nor the particle size distribution. TEM investigation confirmed that particles with diameters ranging from 3 to 10 nm are homogeneously decorating the whole external surface of the CNTs (Figure 5). Consequently, it appears that the physical properties of solvent A do not have a significant impact on the final material when synthesized under our conditions.

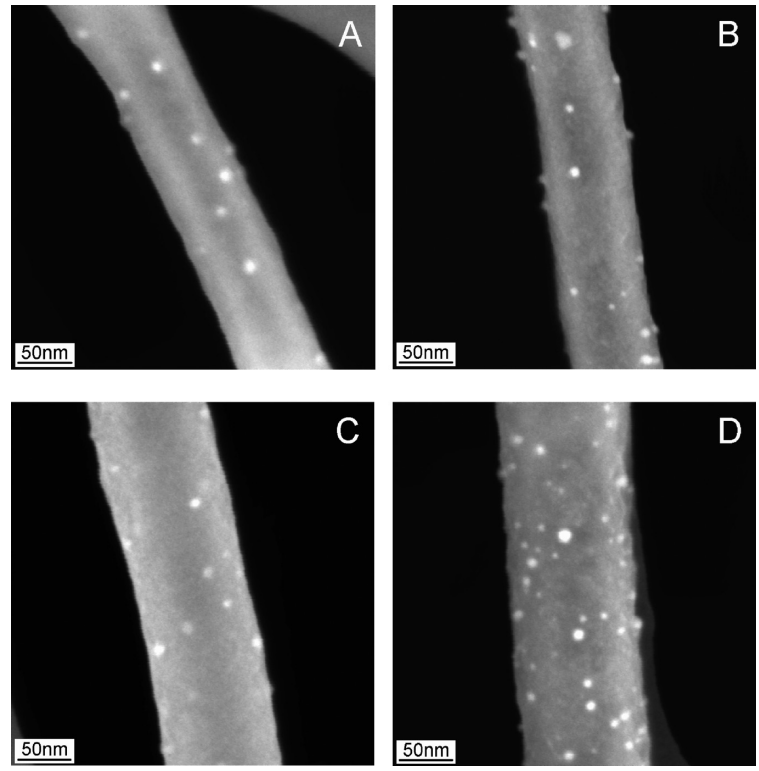

Figure 4. SEM images of 1 wt % Ni/CNT samples "metal outside" prepared with solvents of various boiling point and solubility in water (A, benzene; B, ethanol; C, octane; D, *N*,*N*-dimethylformamide). The nature of the solvent affects neither the dispersion nor the average particle size.

TABLE 1. Physical Properties of the Organic Solvents Used for the Selective Deposition of Metal Nanoparticles on the Outer Surface of the CNTs. Values Were Taken from the CRC Handbook of Chemistry and Physics[41]

solvent	γ (mN · m^{-1})[a]	solubility in water (wt %)	boiling point (K)
water	71.99	/	373
octane	21.14	7.1×10^{-5}	398
ethylbenzene	28.75	1.6×10^{-2}	409
benzene	28.22	1.78×10^{-1}	353
trichloromethane	26.67	8.0×10^{-1}	334
ethylene glycol	47.99	soluble	469
N,*N*-dimethylformamide	37.10	soluble	426
ethanol	21.82	soluble	351
tetrahydrofuran	26.4	soluble	339

[a]Surface tension at 298 K.

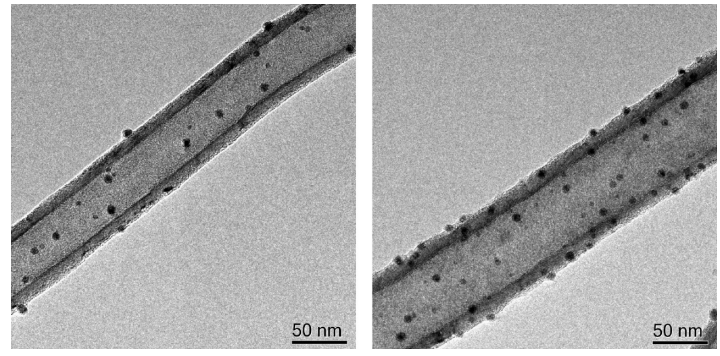

Figure 5. TEM images obtained for the samples "metal outside" prepared with different organic solvents: ethylene glycol (left), tetrahydrofuran (right). The nature of the solvent affects neither the dispersion nor the particle size.

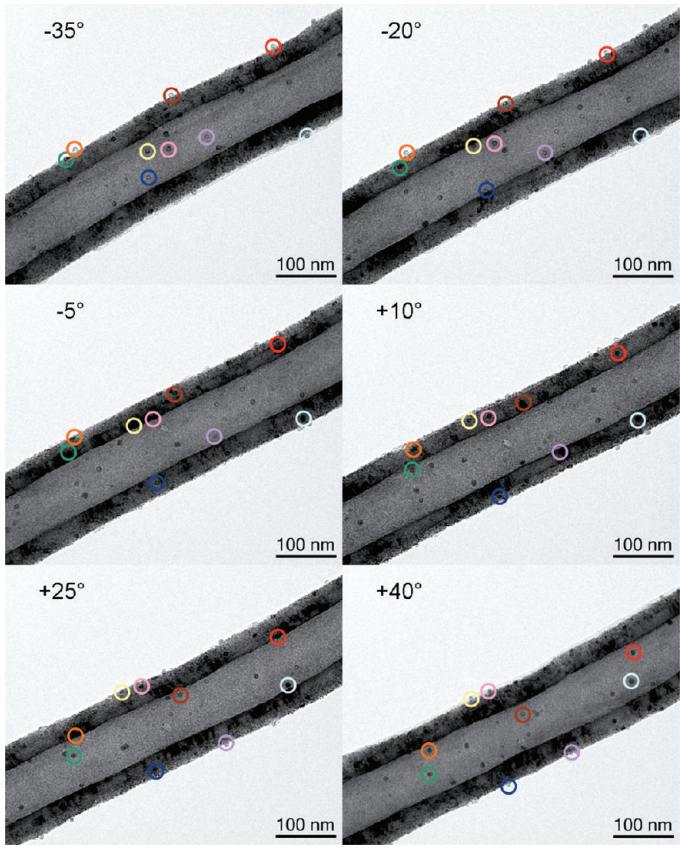

Figure 6. TEM tilt series obtained by tilting the sample "metal outside" prepared with octane from −35° to +40°.

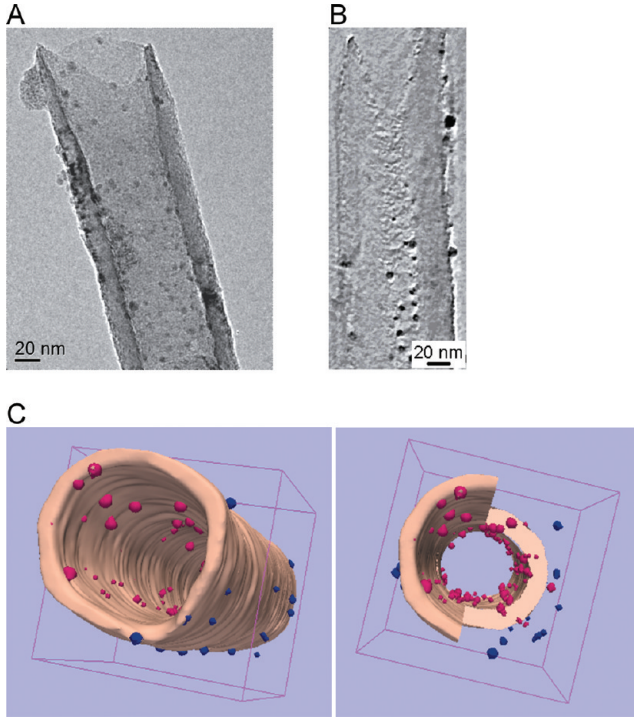

Figure 7. (A) Typical 2D-TEM image of the sample "metal inside", used to reconstruct its volume. (B) Longitudinal section through the reconstructed volume. (C) Modeling of the reconstructed volume: (pink) carbon nanotube, (red) Ni particles inside the tube, (blue) Ni particles on the external surface).

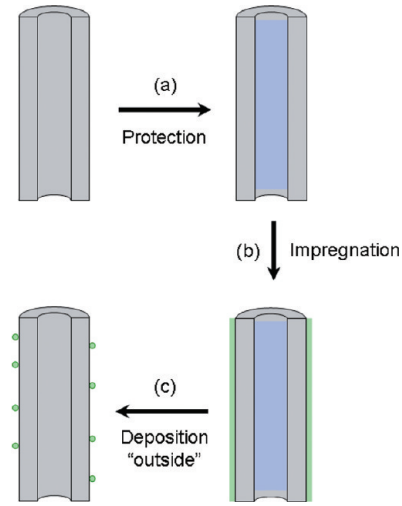

Scheme 2. Schematic view of a longitudinal cross section of a carbon nanotube during the different steps for the selective deposition of nanoparticles *outside* CNTs: (a) impregnation with the organic solvent to protect the inner tubule from metal deposition; (b) impregnation with the aqueous solution containing the metal precursor; (c) after drying, calcination, and reduction, metal particles are decorating the outer surface of the CNT with a high selectivity.

Additional experiments that are not reported here however show that the boiling point of solvent A has an effect if the initial drying step is done at higher temperature, for example, at a temperature close to or higher than the boiling point of the solvent. In this case, solvent A evaporates and therefore no longer protects the inner channel. The aqueous solution containing the Ni then goes into the nanotube by capillarity, thus leading to a loss of selectivity. From Table 1, it is also worth noting that other parameters, like the polaritiy of solvent A, do not seem to play a role during the synthesis. The similar dispersion and size distribution of the Ni particles for all samples make us conclude that the organic solvent neither chemically modifies the external surface of the CNTs nor interacts with the Ni-containing aqueous solution. The organic solvent seems to go into the nanotube, fill the tubule, and remain inside as expected.

SEM and TEM together provide clear information about metal dispersion and particle size distribution. TEM can also provide additional information about the location of the particles inside/outside the CNTs when tilting the sample, that is, by rotating one CNT around its axis and taking a series of images. Tilting the sample allows images to be taken from the same area but with different perspectives, giving reliable information on the location of the particles: particles inside the tube will move but their motion will be restricted to the inner tubule; particles that are in the middle of the tube but outside will progressively move toward the outer wall and will finally reach it and cross it (Figure 6). A video made of 16 images obtained by tilting the sample from −35° to +40° with steps of 5° can be found as Supporting Information.

Quantitative Analysis of the Nanoparticles Ratio inside/outside the CNTs. 3D-TEM, as for every tomographic technique, relies on the volume reconstruction of an object through one or several projection series. 3D electron microscopy has been used mainly in biology.[37] Since a few years, some research teams working in the field of materials science try to explore its possibilities and advantages, for example for determining the 3D structure of catalysts.[38,39] Shortly, it consists in taking a series of TEM images when tilting the specimen with respect to the electron beam around a tilt axis. Once the series of projections recorded, the reconstruction of the object is calculated by specific algorithms and finally it can give rise to a 3D model of the sample structure. In our case, the use of this technique gives statistical data about the location of the nanoparticles and their size, as well as distinguishing between the inner and outer parts of the CNTs in order to estimate the ratio of the nanoparticles inserted in the tubes.

To estimate more accurately the efficiency of the filling process and to validate the hypothesis of a high selectivity inside/outside of the particles, we performed 3D-TEM analyses of representative CNTs for the two types of samples. For the sample "metal inside", a typical 2D image used to reconstruct the volume of the whole object is shown in Figure 7A. From such a bright-field image, it is obviously not possible to determine the location of the Ni nanoparticles, but even their observation and analysis is quite difficult, due to a difference in mass−thickness contrast not high enough between Ni and C. In the sections through the reconstructed volume (a longitudinal section is presented in Figure 7B), the individual analysis of their size is facilitated by the increase of the signal-to-noise ratio due to the redundancy of information coming from several images. However, the main goal of this technique here is related to the estimation of the ratio inside/outside of the Ni particles. Using the 3D positions of these particles with respect to the inner and outer surfaces of the tube obtained by modeling, we separated the inside/outside particles (in red and in blue in Figure 7C, respectively) and calculated the corresponding ratio: for this sample, near 75% of the Ni particles are thus located inside the tube. According to this ratio, one could state that even by using the two-step impregnation it is not always possible to reach a totally selective decoration, as some residual metal particles still remain on the outer surface of the support. However, it is noteworthy that by using the present deposition technique a significant improvement was achieved compared to the classical incipient wetness impregnation method,[32] that is, 75% of filling instead of 50%.

We performed a similar 3D-TEM analysis on the sample "metal outside" prepared with benzene. Once again, the precise localization of all the nanoparticles is difficult from a 2D-TEM picture, even if the successive TEM observations at different tilt angles suggest a preferentially outside decoration of the tube. A typical projection of the object and several sections through the volume as obtained from the reconstruction are presented in Figure 8. By extracting the nanoparticles and nanotube contributions from the total volume, we obtained the exact position of the nanoparticles with respect to the outer surface and estimated thus the ratio inside/outside in the case of the two-step impregnation process proposed here. For this sample, the selectivity of particles deposited on the outer surface is rather high, close to 85%. The higher selectivity for the external deposition was attributed to the fact that the aqueous solution evaporation on the outer surface was more efficient, as all the solution is in direct contact with air. The evaporation of the organic solvent is much slower as it fills the tubule and it is in contact with air only at the tube tips. For both types of samples, "metal inside" and "metal outside", the particle size ranges from 3 to 7 nm for the particles inside and 4 to 9 nm for the particles outside. These values are inline with the SEM and TEM observations (Figures 3−6) and confirm that the nature of the solvent affects neither the dispersion nor the average particle size.

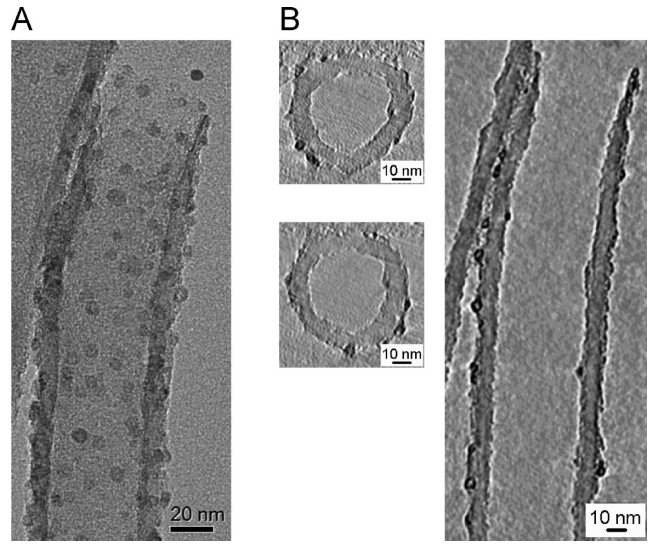

Figure 8. (A) One of the 2D-TEM images from the tilts series used for 3D-TEM analysis of the sample "metal outside" prepared with benzene. (B) Transeversal and a longitudinal sections through the volume obtained by reconstruction.

CONCLUSION

Selective, localized deposition of metal nanoparticles on carbon nanotubes is possible by using a combination of organic and aqueous solvents. By testing different solvents we demonstrated that other parameters like the miscibility with water and the boiling point have no crucial effect in our synthesis conditions. The difference in the liquid/solid interface energies of both solvents with the CNT surface is a crucial parameter. This method allows the avoidance of any additional step of selected functionalization which is difficult, time-consuming, and altering the surface chemistry of

the CNT walls. The two-step biphasic impregnation described in the present work makes it possible to prepare new materials for catalysis, magnetism, and electronics where the inner and outer surface of the CNTs would be decorated or covered with different materials, that is, a layered structure.

EXPERIMENTAL SECTION

Carbon Nanotube Support. Carbon nanotubes were supplied by Pyrograf Products, Inc. (OH). Their initial specific surface area, measured by N_2 adsorption at liquid N_2 temperature, is 55 m^2/g. The CNTs were treated at 373 K with concentrated nitric acid (65% HNO_3) for 16 h in order to remove the residual catalyst and carbon impurities and to functionalize the nanotube inner and outer surfaces. Typically, 10 g of CNTs were treated with 500 mL of concentrated nitric acid under vigorous stirring (500 rpm) in a 1 L round bottomed flask equipped with a condenser. After 16 h, the mixture was allowed to cool down to room temperature. The CNTs were then filtered on a Büchner and were extensively rinsed with distilled water (at least 1 L) until reaching a neutral pH.

Nanohybrids Synthesis. The porous volume of the support was determined by impregnation of 1 g of CNTs with distilled water until reaching the incipient wetness. It was found to be 6 mL/g_{CNT}. For the reference 1 wt % Ni/CNT sample prepared by incipient wetness, 50 mg of nickel nitrate hexahydrate ($Ni(NO_3)_2 \cdot 6H_2O$, Acros) were first dissolved in 6 mL of distilled water. The solution was then slowly added to 1 g of CNTs using a Pasteur pipet, while continuously stirring the paste with a glass stick. The mixture was dried at 323 K for 10 h. Then, it was calcined in static air at 623 K for 2 h (heating ramp: 10 °C/min) in order to decompose the nickel precursor and form nickel oxide particles. Finally, the sample was reduced in flowing hydrogen (50 mL/min) at 673 K for 2 h (heating ramp: 10 °C/min). The sample with metal nanoparticles selectively deposited inside the CNTs was synthesized as follows: 1 g of CNTs was first impregnated with 4 mL of an ethanolic solution containing the nickel nitrate precursor (50 mg of nickel nitrate hexahydrate dissolved in 4 mL of ethanol). The volume of the solution was set to be lower than the porous volume of the CNT (4 mL/g_{CNT} instead of 6 mL/g_{CNT}). In a second step, 3 mL of pure distilled water are then added (see Scheme 1). The paste was dried, calcined, and reduced in the same conditions as the reference sample. For the samples with Ni nanoparticles selectively deposited outside, 1 g of CNTs was first impregnated with 6 mL of one of the organic solvents listed in Table 1. In a second step, 4 mL of an aqueous solution containing the Ni precursor were added. Drying, calcination, and reduction were performed in the same conditions as for the reference sample. All solvents were ACS grade and used without further purification. Additional comments concerning the synthesis methods are found in the Results and Discussion section.

Nanohybrids Characterization. The zeta potential of the functionalized CNTs was measured with a Malvern Zetasizer (Zen 3600) at a constant temperature of 298 K. Functionalized CNTs were dispersed in distilled water by ultrasonication. The pH of the CNT solution was decreased from 9.5 to 1.5 in steps of 0.2 by adding 0.25 M hydrochloric acid. XPS measurements were carried out using a modified LHS/SPECS EA200 MCD system equipped with a Mg Kα source (1253.6 eV, 168 W). The binding energy scale of the system was calibrated using Au $4f_{7/2}$ = 84.0 eV and Cu $2p_{3/2}$ = 932.67 eV from foil samples. The powder samples were placed as is in a stainless steel sample holder with a 0.6 mm deep rectangular well covering an area of (12 × 8) mm^2. SEM images were acquired with a Hitachi S4800 FEG microscope equipped with SE (upper and lower), YAG-BSE and TE detectors, as well as an EDS system for elemental analysis. The samples were typically dispersed on a conductive carbon tape. SE images were acquired at different accelerating voltages, that is, 2 and 15 kV. Images acquired at 2 kV are more surface sensitive as the primary electrons have an energy too low to penetrate deeply into the sample. The image is mainly generated from secondary electrons emitted from the surface of the sample. The samples were also dispersed on holey carbon coated Cu grids to acquire images in transmitted electron (TE) mode. Conventional high resolution TEM images were acquired with a Philips CM 200 LaB_6 microscope operated at 200 kV. The tilt series for 3D-TEM experiments were recorded in bright-field mode on a TECNAI F20 microscope, running at 200 kV high-voltage with a specific high tilt holder allowing a maximum tilt angle of ±70° around an axis perpendicular to the beam direction. The acquisition process was performed using the FEI eXplore3D acquisition software which is able to change automatically the tilt angle, to correct defocus and the shift of the object, and to record and store 2D images. With tilt angles ranging from −65° to 65° and 2° increments between −30° and 30° and 1° elsewhere, the tilt series consists of 101 images. A 2048 × 2048 pixels cooled CCD array detector was used to store these images with an exposure time of 1 s per image. No apparent irradiation damage on the specimen was observed during the total acquisition time of the tilt series. The reconstructed volumes were calculated using the weighted back-projection algorithm implemented in the IMOD software.[40] The spatial resolution in the reconstructions estimated for our acquisition parameters is about 2 nm along the electron beam and 1.5 nm in the perpendicular directions. To determine the exact positions of the nanoparticules with respect to the inner and outer surface of the nanotube, we have modeled the volume using a segmentation procedure based on the gray-level intensities of the voxels.

Acknowledgment. The authors thank C. Hess and O. Timpe for performing XPS and ZP measurements, respectively. H. Möhwald is warmly thanked for his advice. This work has been carried out within the framework of ELCASS (European Laboratory for Catalysis and Surface Sciences).

Supporting Information Available: Scheme showing the variety of oxygen-containing groups existing on the surface of the functionalized CNTs, O 1s XP spectrum, TG/TDS and ZP results measured for the functionalized CNTs, movies obtained from TEM tilt series. This material is available free of charge *via* the Internet at http://pubs.acs.org.

REFERENCES AND NOTES

1. Endo, M.; Strano, M.; Ajayan, P., Potential Applications of Carbon Nanotubes. In *Carbon Nanotubes*; Jorio, A., Dresselhaus, G., Dresselhaus, M. S., Eds.; Springer-Verlag: Berlin/Heidelberg, Germany, 2008; pp 13−61.
2. Serp, P.; Corrias, M.; Kalck, P. Carbon Nanotubes and Nanofibers in Catalysis. *Appl. Catal., A* **2003**, *253*, 337–358.
3. Zhang, J.; Liu, X.; Blume, R.; Zhang, A.; Schlögl, R.; Su, D. S. Surface-Modified Carbon Nanotubes Catalyze Oxidative Dehydrogenation of *n*-Butane. *Science* **2008**, *322*, 73–77.
4. Niyogi, S.; Hamon, M. A.; Hu, H.; Zhao, B.; Bhowmik, P.; Sen, R.; Itkis, M. E.; Haddon, R. C. Chemistry of Single-Walled Carbon Nanotubes. *Acc. Chem. Res.* **2002**, *35*, 1105–1113.
5. Hirsch, A.; Vostrowsky, O., Functionalization of Carbon Nanotubes. In *Functional Organic Materials*; Müller, T. J. J., Bunz, U. H. F., Eds.; Wiley-VCH: Weinheim, Germany, 2007.
6. Ajayan, P. M.; Ebbesen, T. W.; Ichihashi, T.; Iijima, S.; Tanigaki, K.; Hiura, H. Opening Carbon Nanotubes with Oxygen and Implications for Filling. *Nature* **1993**, *362*, 522–525.
7. Tsang, S. C.; Chen, Y. K.; Harris, P. J. F.; Green, M. L. H. A Simple Chemical Method of Opening and Filling Carbon Nanotubes. *Nature* **1994**, *372*, 159–162.
8. Terrones, M.; Filho, A.; Rao, A., Doped Carbon Nanotubes: Synthesis, Characterization and Applications. In *Carbon Nanotubes*; Jorio, A., Dresselhaus, G., Dresselhaus, M. S., Eds.; Springer-Verlag: Berling/Heidelberg, Germany, 2008; pp 531−566.

9. Costa, P. M. F. J.; Sloan, J.; Rutherford, T.; Green, M. L. H. Encapsulation of RexOy Clusters within Single-Walled Carbon Nanotubes and Their *in Tubulo* Reduction and Sintering to *Re* Metal. *Chem. Mater.* **2005**, *17*, 6579–6582.
10. Wu, H.-Q.; Wei, X.-W.; Shao, M.-W.; Gu, J.-S.; Qu, M.-Z. Preparation of Fe−Ni Alloy Nanoparticles Inside Carbon Nanotubes *via* Wet Chemistry. *J. Mater. Chem.* **2002**, *12*, 1919–1921.
11. Kim, B. M.; Qian, S.; Bau, H. H. Filling Carbon Nanotubes with Particles. *Nano Lett.* **2005**, *5*, 873–878.
12. Chen, S.; Wu, G.; Sha, M.; Huang, S. Transition of Ionic Liquid [bmim][PF6] from Liquid to High-Melting-Point Crystal When Confined in Multiwalled Carbon Nanotubes. *J. Am. Chem. Soc.* **2007**, *129*, 2416–2417.
13. Schulte, K.; Swarbrick, J. C.; Smith, N. A.; Bondino, F.; Magnano, E.; Khlobystov, A. N. Assembly of Cobalt Phthalocyanine Stacks Inside Carbon Nanotubes. *Adv. Mater.* **2007**, *19*, 3312–3316.
14. Bazilevsky, A. V.; Sun, K.; Yarin, A. L.; Megaridis, C. M. Room-Temperature, Open-Air, Wet Intercalation of Liquids, Surfactants, Polymers and Nanoparticles within Nanotubes and Microchannels. *J. Mater. Chem.* **2008**, *18*, 696–702.
15. Monthioux, M. Filling Single-Wall Carbon Nanotubes. *Carbon* **2002**, *40*, 1809–1823.
16. Zhang, J.; Hu, Y.-S.; Tessonnier, J.-P.; Weinberg, G.; Maier, J.; Schlögl, R.; Su, D. S. CNFs@CNTs: Superior Carbon for Electrochemical Energy Storage. *Adv. Mater.* **2008**, *20*, 1450–1455.
17. Sloan, J.; Kirkland, A. I.; Hutchison, J. L.; Green, M. L. H. Structural Characterization of Atomically Regulated Nanocrystals Formed within Single-Walled Carbon Nanotubes Using Electron Microscopy. *Acc. Chem. Res.* **2002**, *35*, 1054–1062.
18. Tessonnier, J.-P.; Pesant, L.; Ehret, G.; Ledoux, M. J.; Pham-Huu, C. Pd Nanoparticles Introduced Inside Multi-Walled Carbon Nanotubes for Selective Hydrogenation of Cinnamaldehyde into Hydrocinnamaldehyde. *Appl. Catal., A* **2005**, *288*, 203–210.
19. Ledoux, M. J.; Vieira, R.; Pham-Huu, C.; Keller, N. New Catalytic Phenomena on Nanostructured (Fibers and Tubes) Catalysts. *J. Catal.* **2003**, *216*, 333–342.
20. Pan, X.; Fan, Z.; Chen, W.; Ding, Y.; Luo, H.; Bao, X. Enhanced Ethanol Production Inside Carbon-Nanotube Reactors Containing Catalytic Particles. *Nat. Mater.* **2007**, *6*, 507–511.
21. Castillejos, E.; Debouttière, P.-J.; Roiban, L.; Solhy, A.; Martinez, V.; Kihn, Y.; Ersen, O.; Philippot, K.; Chaudret, B.; Serp, P. An Efficient Strategy to Drive Nanoparticles into Carbon Nanotubes and the Remarkable Effect of Confinement on Their Catalytic Performance. *Angew. Chem., Int. Ed.* **2009**, *48*, 2529–2533.
22. Schlögl, R. Carbons. In *Handbook of Heterogeneous Catalysis*; Ertl, G., Knözinger, H., Schüth, F., Weitkamp, J., Eds.; Wiley-VCH Verlag: Weinheim, Germany, 2007.
23. Derouane, E. G. Zeolites as Solid Solvents. *J. Mol. Catal. A: Chem.* **1998**, *134*, 29–45.
24. Caro, J. Fluid Flow. In *Handbook of Porous Solids*; Schüth, F., Sing, K. S. W., Weitkamp, J., Eds.; Wiley-VCH Verlag: Weinheim, Germany, 2002, pp 352−370.
25. Noy, A.; Park, H. G.; Fornasiero, F.; Holt, J. K.; Grigoropoulos, C. P.; Bakajin, O. Nanofluidics in Carbon Nanotubes. *Nano Today* **2007**, *2*, 22–29.
26. Trens, P.; Tanchoux, N.; Galarneau, A.; Fajula, F. New Evidence of Confinement Effects in Mesoporous Materials and the Definition of Confined Pitzer Acentric Factors. *J. Phys. Chem. B* **2005**, *109*, 16415–16420.
27. Ma, H.; Wang, L.; Chen, L.; Dong, C.; Yu, W.; Huang, T.; Qian, Y. Pt Nanoparticles Deposited over Carbon Nanotubes for Selective Hydrogenation of Cinnamaldehyde. *Catal. Commun.* **2007**, *8*, 452–456.
28. Lee, K. M.; Li, L.; Dai, L. Asymmetric End-Functionalization of Multi-Walled Carbon Nanotubes. *J. Am. Chem. Soc.* **2005**, *127*, 4122–4123.
29. Jiang, L.; Gao, L. Modified Carbon Nanotubes: an Effective Way to Selective Attachment of Gold Nanoparticles. *Carbon* **2003**, *41*, 2923–2929.
30. Chen, W.; Pan, X.; Bao, X. Tuning of Redox Properties of Iron and Iron Oxides *via* Encapsulation within Carbon Nanotubes. *J. Am. Chem. Soc.* **2007**, *129*, 7421–7426.
31. Winter, F.; Leendert Bezemer, G.; van der Spek, C.; Meeldijk, J. D.; Jos van Dillen, A.; Geus, J. W.; de Jong, K. P. TEM and XPS Studies to Reveal the Presence of Cobalt and Palladium Particles in the Inner Core of Carbon Nanofibers. *Carbon* **2005**, *43*, 327–332.
32. Ersen, O.; Werckmann, J.; Houlle, M.; Ledoux, M. J.; Pham-Huu, C. 3D Electron Microscopy Study of Metal Particles inside Multiwalled Carbon Nanotubes. *Nano Lett.* **2007**, *7*, 1898–1907.
33. Ros, T. G.; van Dillen, A. J.; Geus, J. W.; Koningsberger, D. C. Surface Oxidation of Carbon Nanofibres. *Chem.—Eur. J.* **2002**, *8*, 1151–1162.
34. Xia, W.; Wang, Y.; Bergstraer, R.; Kundu, S.; Muhler, M. Surface Characterization of Oxygen-Functionalized Multi-Walled Carbon Nanotubes by High-Resolution X-ray Photoelectron Spectroscopy and Temperature-Programmed Desorption. *Appl. Surf. Sci.* **2007**, *254*, 247–250.
35. Farrauto, R. J.; Bartholomew, C. H. *Fundamentals of Industrial Catalytic Processes*; Blackie Academic & Professional: London, 1997.
36. Ebbesen, T. W. Wetting, Filling and Decorating Carbon Nanotubes. *J. Phys. Chem. Solids* **1996**, *57*, 951–955.
37. Koster, A. J.; Grimm, R.; Typke, D.; Hegerl, R.; Stoschek, A.; Walz, J.; Baumeister, W. Perspectives of Molecular and Cellular Electron Tomography. *J. Struct. Biol.* **1997**, *120*, 276–308.
38. Midgley, P. A.; Weyland, M. 3D Electron Microscopy in the Physical Sciences: The Development of *Z*-Contrast and EFTEM Tomography. *Ultramicroscopy* **2003**, *96*, 413–431.
39. de Jong, K. P.; Koster, A. J. Three-Dimensional Electron Microscopy of Mesoporous Materials—Recent Strides Towards Spatial Imaging at the Nanometer Scale. *ChemPhysChem* **2002**, *3*, 776–780.
40. Mastronarde, D. N. Automated Electron Microscope Tomography using Robust Prediction of Specimen Movements. *J. Struct. Biol.* **2005**, *152*, 36–51.
41. Lide, D. R. *CRC Handbook of Chemistry and Physics*; CRC Press: Boca Raton, FL, 2003.